

# Characteristics of the Interaction of a Synthetic Human Tristetraprolin Tandem Zinc Finger Peptide with AU-rich Element-containing RNA Substrates\*

Received for publication, February 5, 2003, and in revised form, March 7, 2003  
Published, JBC Papers in Press, March 14, 2003, DOI 10.1074/jbc.M301290200

Perry J. Blackshear<sup>†§¶\*</sup>, Wi S. Lai<sup>‡</sup>, Elizabeth A. Kennington<sup>‡</sup>, Gary Brewer<sup>‡‡</sup>,  
Gerald M. Wilson<sup>‡‡§§</sup>, Xiaoju Guan<sup>||</sup>, and Pei Zhou<sup>||</sup>

From the <sup>‡</sup>Laboratory of Signal Transduction and the <sup>§</sup>Office of Clinical Research, National Institute of Environmental Health Sciences, National Institutes of Health, Department of Health and Human Services, Research Triangle Park, North Carolina 27709, the Departments of <sup>¶</sup>Medicine and <sup>||</sup>Biochemistry, Duke University Medical Center, Durham, North Carolina 27710, and the <sup>‡‡</sup>Department of Molecular Genetics, Microbiology, and Immunology, University of Medicine and Dentistry of New Jersey-Robert Wood Johnson Medical School, Piscataway, New Jersey 08854

Tristetraprolin (TTP) and its two known mammalian family members are tandem CCCH zinc finger proteins that can bind to AU-rich elements (AREs) in cellular mRNAs and destabilize those transcripts, apparently by initiating their deadenylation. Previous studies have shown that the ~70-amino acid tandem zinc finger domain of TTP is required and sufficient for RNA binding, and that the integrity of both zinc fingers is also required. However, little is known about the kinetics or structure of the peptide-RNA interaction, in part because of difficulties in obtaining soluble recombinant protein or peptides. We characterized the binding of a synthetic 73-amino acid peptide from human TTP to the tumor necrosis factor (TNF) ARE by gel mobility shift analyses and fluorescence anisotropy experiments. Both types of studies yielded a peptide-RNA dissociation constant of ~10 nM. Surprisingly, we found that the “footprint” from the TNF ARE required for peptide binding was only ~9 bases and that two molecules of peptide could bind to probes containing as little as 19 bases. An identical recombinant peptide exhibited gel shift characteristics similar to those of the synthetic peptide. NMR analysis of the <sup>15</sup>N-labeled recombinant peptide suggested that its first zinc finger was structured in solution but that the second was not. The titration of oligonucleotides representing 17, 13, and even 9 bases of the TNF ARE caused an essentially identical, dramatic shift of existing resonances, and the appearance of new resonances in the peptide spectra, so that all amino acids could be assigned. These data suggest that this TTP peptide-RNA complex is structured in solution and might be amenable to NMR structure determination.

Tristetraprolin (TTP)<sup>1</sup> is the prototype of a small family of eukaryotic CCCH tandem zinc finger proteins (see Ref. 1 for recent review). In mammals, there are three known members of this protein family, whereas fish and frogs express a fourth member that seems to consist of a group of closely related proteins (2–4). The characteristic tandem zinc finger domain of these proteins consists of two zinc fingers with 18 amino acids between fingers, strict intrafinger spacing of Cx8Cx5Cx3H, and a characteristic sequence motif leading into each finger of R(K)YKTEL or a closely related variant.

Studies in TTP knockout mice and cells derived from them revealed that TTP acts in normal physiology to regulate the synthesis and secretion of two clinically important cytokines, tumor necrosis factor (TNF) and granulocyte-macrophage colony-stimulating factor (GM-CSF) (5–9). The increased secretion of these cytokines in the TTP knockout mice was secondary to increased steady state levels of their mRNAs, which in turn was caused by excessive stabilization of the transcripts. TTP was found to confer instability on these two transcripts by binding to the so-called class II AREs contained within the 3'-untranslated regions of these mRNAs (7, 10–13). The tandem zinc finger domain was found to be the RNA binding domain, and the invariant cysteine and histidine residues in both fingers were required for mRNA binding. Thus, TTP seems to act in normal physiology to bind to and promote the destruction of the labile transcripts for TNF and GM-CSF.

Subsequent studies have suggested that TTP in some way promotes the earliest step in mRNA turnover in mammalian cells, removal of the poly(A) tail, or deadenylation. Studies in bone marrow-derived stromal cells from TTP-deficient mice established that deadenylation of GM-CSF mRNA was defective in those cells (8), leading to the marked stabilization of the fully polyadenylated GM-CSF transcripts. These data represented strong evidence that TTP exerted its destabilizing effect on ARE-containing mRNAs by first binding to the ARE and then promoting deadenylation; the deadenylated mRNA body would then decay by other mechanisms. The two other known mammalian members of the TTP protein family, ZFP36L1 and ZFP36L2, can exert TTP-like effects on mRNA stability in transfection studies in intact cells (13), and promote removal of the poly(A) tail in a cell-free deadenylation assay (14); however,

\* This work was supported in part by Grant R01-CA52443 from NCI, National Institutes of Health, a grant from the Arthritis Foundation (to G. B.) and a Scientist Development Grant from the American Heart Association (to G. M. W.). P. Z. was supported in part by the Duke University Junior Faculty Start-up Fund and the Whitehead Institute. G. B. is an Elsie Eggert/American Heart Association Research Fellow. The costs of publication of this article were defrayed in part by the payment of page charges. This article must therefore be hereby marked “advertisement” in accordance with 18 U.S.C. Section 1734 solely to indicate this fact.

\*\* To whom correspondence should be addressed: A2-05, NIEHS, 111 Alexander Dr., Research Triangle Park, NC 27709. Tel.: 919-541-4899; Fax: 919-541-4571; E-mail: black009@niehs.nih.gov.

§§ Present address: Dept. of Biochemistry and Molecular Biology, University of Maryland School of Medicine, Baltimore, MD 21201.

<sup>1</sup> The abbreviations used are: TTP, tristetraprolin; TNF, tumor necrosis factor; ARE, AU-rich element; GM-CSF, granulocyte-macrophage colony-stimulating factor; TZF, tandem zinc finger; HSQC, heteronuclear single quantum coherence; HPLC, high performance liquid chromatography.



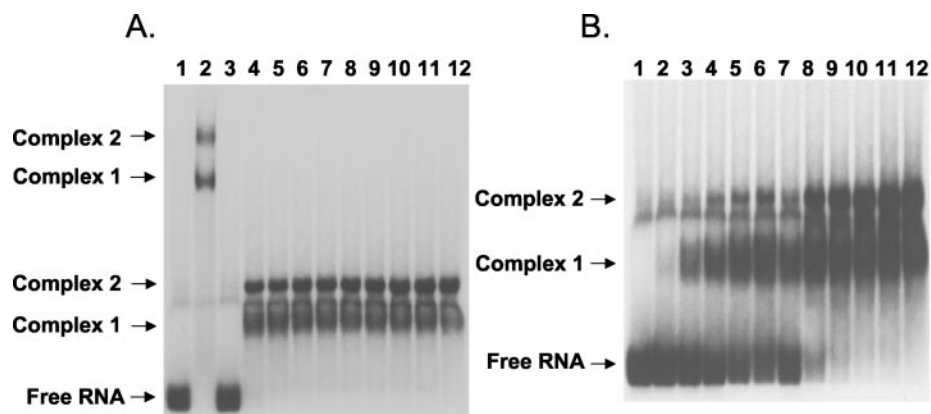


FIG. 2. Binding of 24b ARE probe to various concentrations of the TTP73 peptide. Binding reactions and gel shift analyses were carried out as described under "Experimental Procedures." A, migration position of probe alone (Free RNA; lane 1), the binding of the probe to full-length, epitope-tagged TTP in a cytosolic 293 cell extract (lane 2; complexes 1 and 2); and the binding of the probe to various concentrations of the TTP73 peptide, which also formed complexes 1 and 2 lower in the gel. Peptide concentrations were as follows: lane 3, probe alone; lane 4, 100 nM TTP73; lane 5, 200 nM; lane 6, 300 nM; lane 7, 400 nM; lane 8, 500 nM; lane 9, 600 nM; lane 10, 700 nM; lane 11, 800 nM; and lane 12, 1.0  $\mu$ M. B, results of a similar binding study with lower concentrations of peptide. In lane 1 was probe alone incubated with buffer; lane 2, 6 nM peptide; lane 3, 10 nM; lane 4, 20 nM; lane 5, 40 nM; lane 6, 60 nM; lane 7, 80 nM; lane 8, 100 nM; lane 9, 200 nM; lane 10, 400 nM; lane 11, 600 nM; lane 12, 800 nM. The migration positions of the probe alone (Free RNA) and of complexes 1 and 2 are indicated. The autoradiographs were intentionally overexposed to investigate the possible presence of larger complexes.

(18), except that  $\text{ZnCl}_2$  (5  $\mu$ M) was added to protein samples 30 min before the anisotropy measurements. Because TTP73 binding did not alter the fluorescence quantum yield of the labeled RNA substrates (Fig. 5B), total anisotropy ( $A_t$ ) was interpreted based on direct fractional contributions from each fluorescing species (bound versus free RNA) as described previously (17, 19). Binding affinity was calculated by measuring total anisotropy ( $A_t$ ) across a range of protein ( $P$ ) concentrations ( $n > 30$ ), then resolving these data using a variant of the Hill model, given by Equation 1 (18),

$$A_t = \frac{A_R + A_{PR} K[P]^{n_H}}{1 + K[P]^{n_H}} \quad (\text{Eq. 1})$$

where  $K$  is the equilibrium association constant ( $= 1/K_d$ ),  $n_H$  is the Hill coefficient, and  $A_R$  and  $A_{PR}$  represent the intrinsic anisotropy values of the free and protein-associated fluorescein-labeled RNA substrates, respectively. Although individual binding steps in oligomerization mechanisms cannot be defined by this algorithm (20), it will detect significant deviation from a single-site binding model (i.e.  $n_H = 1$ ).  $A_R$  was defined by the anisotropy of RNA substrates measured in the absence of TTP73 ( $n \geq 3$ ), whereas all other constants were solved by non-linear least squares regression using Prism v.2.0 (GraphPad Software, San Diego, CA).

**Expression and Purification of Biosynthetic TTP73**—The TZF domain of human TTP (residues 102–174 of GenBank accession number NP\_003398.1) was cloned into the pET30a(+) vector (Novagen Inc., Madison, WI) between the *Nde*I and *Bam*HI sites. The encoded sequence was identical to that of peptide TTP73; no purification tags were used, and no mutant amino acids were inserted into the sequence. The expression vector was transformed into BL21(DE3)STAR competent cells (Invitrogen) containing an isopropyl-D-thiogalactoside-inducible T7 RNA polymerase gene. The transformed cells were grown in LB and induced with 1 mM isopropyl-D-thiogalactoside and 100  $\mu$ M  $\text{ZnSO}_4$  (final concentration) when the  $A_{600}$  reached 0.7. The induced cells were allowed to grow for an additional period of 3 h at 37  $^\circ\text{C}$  and then were harvested by centrifugation. Harvested cells were lysed by passing them through a French pressure cell three times in a lysis buffer containing 25 mM Tris-HCl, pH 8.0, 50 mM NaCl, and 0.1% (v/v)  $\beta$ -mercaptoethanol, and then clarified by centrifugation (70,000  $\times g$  for 60 min at 4  $^\circ\text{C}$ ). In a typical preparation, 30 ml of the clear supernatant containing the TTP peptide was allowed to flow through a 10-ml DEAE column that had previously been equilibrated with a buffer containing 25 mM Tris-HCl, pH 8.0. The flow-through from this column was concentrated to  $\sim$ 10 ml and exchanged into a buffer consisting of 25 mM phosphate, pH 6.5, and 0.1% (v/v)  $\beta$ -mercaptoethanol by ultrafiltration. This solution was then subjected to cation-exchange chromatography on a Source 15S column (Amersham Biosciences) previously equilibrated with a buffer consisting of 25 mM sodium phosphate, pH 6.5, and 0.1% (v/v)  $\beta$ -mercaptoethanol. The peptide was eluted with a gradient of NaCl from 0 to 1 M; the peak elution of the peptide was at 0.5 M NaCl. Fractions containing the peptide were combined, concentrated to 1.8 ml

by using a 3-kDa Centrprep (Millipore Corporation, Bedford, MA), and then further purified by using size-exclusion chromatography using a 1.6  $\times$  60-cm Superdex-75 column (Amersham Biosciences) that had previously been equilibrated in a buffer consisting of 25 mM sodium phosphate, pH 6.5, 150 mM NaCl, and 0.1% (v/v)  $\beta$ -mercaptoethanol. The final preparation of peptide was  $>$  95% pure as determined by SDS-PAGE and Coomassie blue staining; it was also soluble in the gel filtration buffer described above.

For NMR analysis,  $^{15}\text{N}$ - or  $^{15}\text{N}/^{13}\text{C}$ -labeled TTP (102–174) was expressed in M9 minimal medium containing 1.0 g/liter  $^{15}\text{N}/^{13}\text{C}$ -labeled  $^{15}\text{N}/^{13}\text{C}$ -NH $_4$ Cl (Cambridge Isotope Laboratories, Andover, MA) and 2.0 g/liter unlabeled or  $^{13}\text{C}$ -glucose (Cambridge Isotope Laboratories) as the sole nitrogen and carbon sources, and purified as described above. The purified TTP was exchanged into a buffer containing 150 mM NaCl, 25 mM sodium phosphate, pH 6.5, 0.1% (v/v)  $\beta$ -mercaptoethanol, and 5% (v/v) D $_2$ O for NMR analysis.

**NMR Spectroscopy**—All NMR experiments were recorded at 25  $^\circ\text{C}$  on a Varian Inova 600-MHz NMR spectrometer equipped with a 5-mm triple-resonance probe and a shielded Z-gradient unit. Spectra were processed using Felix (Accelrys, San Diego, CA) and analyzed with XEASY (21). HNCACB (22) and CBCA(CO)NH (23) experiments were recorded for the sequential assignment of TTP (102–174). A series of  $^1\text{H}$ - $^{15}\text{N}$  HSQC spectra of  $^{15}\text{N}$ -TTP (102–174) and the various  $^{15}\text{N}$ -TTP(102–174)/RNA oligonucleotide complexes were recorded to study the TTP/ARE RNA interaction.

**RNA Oligonucleotides for NMR**—RNA oligonucleotides were purchased from Dharmacon. Three oligonucleotides were used for NMR: a 17-mer, UUAUUUAUUUAUUUUU, corresponding to bases 1341–1357 of human TNF mRNA (GenBank accession number NM\_000594.2; also identical to a segment of the mouse TNF mRNA, GenBank accession number X02611.1, bases 1309–1325); a 13-mer derived from this 17-mer, UUAUUUAUUUUUU; and a 9-mer derived from this 13-mer, UUAUUUAUU.

## RESULTS

**Gel Shift Analysis**—Exposure of the TTP73 peptide (1  $\mu$ M) to the  $^{32}\text{P}$ -labeled mTNF(1281–1350) probe resulted in the formation of three distinct complexes (Fig. 1A, complexes 1–3). Using a shorter RNA probe (mTNF (1309–1332)), consisting of 24 bases from the mouse TNF core ARE (bp 1309–1332 of GenBank accession number X02611), only complexes 1 and 2 were formed (Fig. 1B). These data suggested a model in which the synthetic peptide was occupying tandem binding sites on the ARE, three in the case of the longer probe, and two in the case of the 24-base probe.

When the shorter probe (mTNF (1309–1332)) was incubated with peptide concentrations from 0.1 to 1  $\mu$ M, the same two probe complexes were observed at all peptide concentrations

tested (Fig. 2A); the two analogous complexes formed with full-length TTP expressed in 293 cells are also shown in Fig. 2A, lane 2). Complex 1 was detectable at peptide concentrations as low as 6 nM (Fig. 2B, lane 2). Filmless autoradiographic analysis of the data on lower band formation (Fig. 2B, complex 1) indicated that half-maximal binding took place at ~8 nM peptide under these conditions. Formation of complex 2 seemed to occur at somewhat higher peptide concentrations. When the amount of radioactivity shifted by both complexes was combined, half-maximal accumulation occurred at ~30 nM peptide. A similar result was obtained when the loss of probe from its original location was measured.

Because mutation of a single key amino acid in either zinc finger abrogates binding of full-length TTP to an ARE probe (13), this binding competence of TTP73 indicates that both zinc fingers were adequately folded to permit high-affinity binding. The data also support the concept of two TTP binding sites on

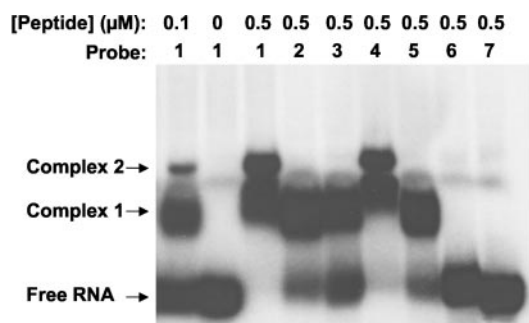
the 24-base ARE probe, suggesting that the footprint of peptide TTP73 was less than 24 bases.

To explore this in greater detail, a series of probes was constructed in which one or more of the A residues within the 24-base ARE were mutated to C residues. Previous studies had indicated that replacement of all six As in this probe with either C or G completely prevented TTP binding (11).<sup>2</sup> Binding of these probes to TTP73 is shown in Fig. 3. Binding of the wild-type ARE-A50 probe (0.1 μM) (Fig. 3, probe 1) to the TTP73 peptide resulted in the formation of an upper complex (complex 2) that contained substantially less radioactivity than the lower complex (complex 1) (Fig. 3, first lane). However, when 0.5 μM peptide was used, the amount of radioactivity in complex 2 increased markedly, and all of the probe was shifted into the gel (Fig. 3, third lane). The migration position of the probe alone is shown in the second lane (Fig. 3).

When probes 2, 3, and 5 were used with the higher peptide concentration (0.5 μM), only complex 1 was formed (Fig. 3), even when the film was relatively overexposed as in Fig. 3. This suggested that binding could occur with the small footprint afforded by the 5' half of probe 3, *i.e.* UUAUUUAAUUU. That only a single complex was formed with these probes suggested that the single A footprint (*i.e.* UUUAAUU) found at the 3'-end of probes 3 and 5 was not sufficient for complex formation. A smaller proportion of probe 3 seemed to be shifted into the gel to form complex 1 than was found with probes 2 and 5 under these conditions, suggesting that the footprints provided by probes 2 and 5 were similar in binding affinity, whereas the footprint provided by probe 3 was of somewhat lower affinity.

When the wild-type probe sequence was changed to include two C residues in the middle (probe 4), both complexes were formed, as seen with the wild-type probe 1. Thus, both the UUAUUUAAUUU and UUUAAUUU 10-base footprints supported peptide binding, and these two footprints, separated by the mutant C-containing sequence, were still adequate to support binding of 2 mol of peptide/mol of probe. This supports a model for the formation of complexes 1 and 2 with the wild-type ARE-A50 probe in which two molecules of peptide are aligned in tandem on a single RNA probe.

As shown previously for intact TTP, there was no detectable binding of the TTP73 peptide to probe 7 (Fig. 3, last lane), in which all six A residues of the 24-base ARE were replaced with



Probes: 1. UUAUUUAAUUUAAUUUAAUUUAAUUU  
 2. UUAUUUAAUUUAAUUUAAUUUAAUUUAAUUU  
 3. UUAUUUAAUUUAAUUUAAUUUAAUUUAAUUU  
 4. UUAUUUAAUUUAAUUUAAUUUAAUUUAAUUU  
 5. UUAUUUAAUUUAAUUUAAUUUAAUUUAAUUU  
 6. UUAUUUAAUUUAAUUUAAUUUAAUUUAAUUU  
 7. UUUUUUUUUUUUUUUUUUUUUUUUUUUUUUU

FIG. 3. Binding of the TTP73 peptide to mutant ARE probes. The gel shift assay was performed with radiolabeled wild-type and mutant ARE probes; the sequences of the ARE portion of the probes are shown, with the original A residues and C substitutions shown in bold. The numbers of the probes correspond to the lane numbers at the top of the gel. The probes were bound to the TTP73 peptide at the concentrations shown at the top of the gel. Complexes 1 and 2, and the positions of the free RNA probes, are indicated.

<sup>2</sup> W. S. Lai and P. J. Blackshear, unpublished data.

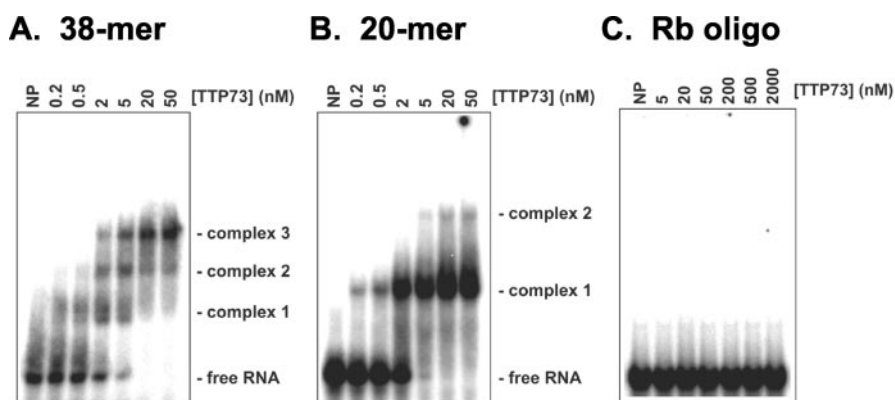
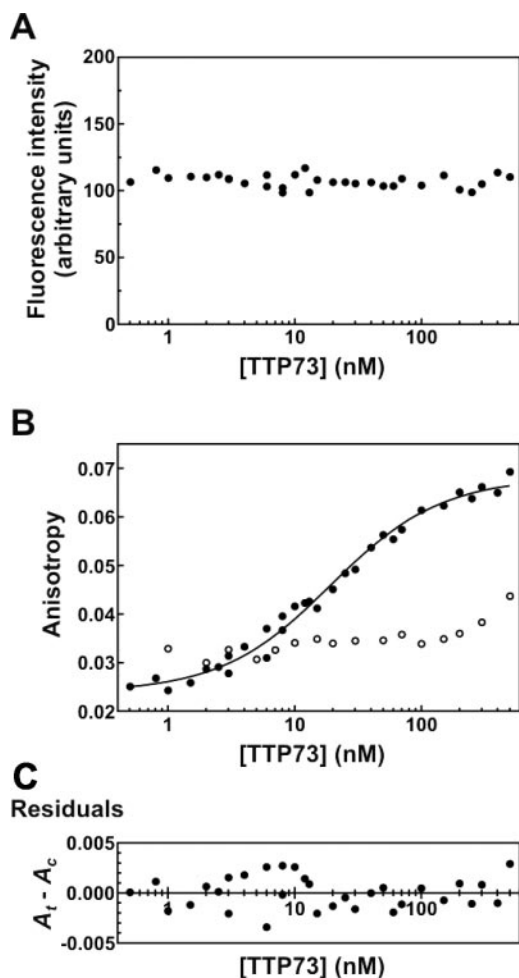


FIG. 4. Gel shift analyses of ARE probes used for fluorescence anisotropy. As described under "Experimental Procedures," a different gel shift assay was performed on radioactive versions of the ARE probes used for fluorescence anisotropy measurements, as described in Fig. 5. A, binding of the 38-mer ARE probe; the peptide concentrations are shown at the top of the autoradiograph, and the positions of complexes 1, 2, and 3, as well as that of the free probe (Free RNA), are indicated. B, a similar gel shift autoradiograph with the shorter, 20-mer ARE probe; in this case, only a single major complex (complex 1) was seen, with a minor complex 2 being barely detectable at higher peptide concentrations (20 and 50 nM). The half-maximal binding concentration of the TTP73 peptide for this probe was 2 nM in this experiment. C, a similar gel shift analysis using the radiolabeled Rb oligonucleotide probe; no shift activity of the TTP73 peptide was observed with this probe, even at concentrations as high as 2 μM.



**FIG. 5. Fluorescence anisotropy of TTP73 binding to the 20-mer ARE probe.** *A*, the effect of the TTP73 peptide at the concentrations shown on the fluorescence intensity of the fluorescent 20-mer ARE probe. There was no effect of the TTP73 peptide on this parameter, even at high concentrations of up to  $1 \mu\text{M}$ . *B*, a plot of fluorescence anisotropy for the 20-mer ARE oligonucleotide (closed circles) as well as for the control  $R\beta$  oligonucleotide (open circles) as functions of TTP73 concentration. The solid line indicates the nonlinear regression solution of these data using the Hill model. The Hill coefficient of this interaction was 0.92. The  $K_d$  was calculated to be 19 nM for this experiment. *C*, the distribution of residuals as a function of TTP73 concentration. The random distribution of residuals indicates no evidence for subsets of the anisotropy data in the regression solution. See the text for further details.

C residues. There was also no detectable binding to probe 6 under these conditions (Fig. 3, *penultimate lane*), indicating that the 6-base footprints UUAUUU (repeated once) and UUUUUU were not adequate for peptide binding.

**Fluorescence Anisotropy Measurements**—First, we tested whether the peptide could bind to the synthetic ARE probes that would be used in these studies. Under different assay conditions (17), the TTP73 peptide slowed the migration of the 38-mer probe, and resulted in the formation of three major complexes (Fig. 4A, *complexes 1–3*). Higher peptide concentrations led to progressively greater appearance of complexes 2 and 3 (Fig. 4A). When the shorter 20-mer probe was used, which contained 19 base from the core TNF ARE, a single major complex was formed (Fig. 4B, *complex 1*), although at considerably higher peptide concentrations, a small amount of complex 2 could be detected (Fig. 4B). Under these assay conditions, half-maximal binding of the probe occurred at  $\sim 2$  nM (Fig. 4B). No binding of the peptide to the control probe  $R\beta$  was seen, even at concentrations as high as  $2 \mu\text{M}$  (Fig. 4C).

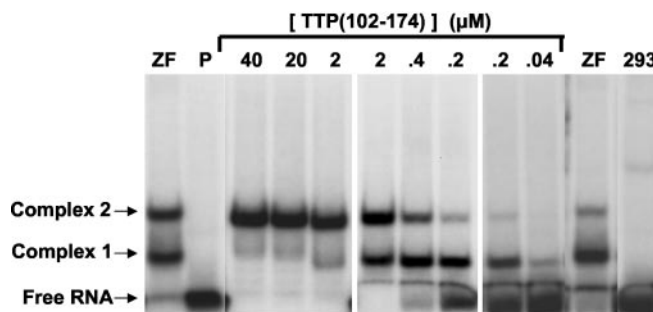


**FIG. 6. Binding of recombinant TTP (102–174) to the 24-base ARE probe.** Gel shift assays were performed using the mTNF(1309–1332) 24-base ARE probe as described in the legend to Figs. 1–3 and under “Experimental Procedures.” *First lane (left)*, formation of complexes 1 and 2 when a cytosolic cell extract ( $5 \mu\text{g}$  of protein) containing expressed TTP zinc finger peptide (ZF) was used as the protein source; a similar assay is shown in the *penultimate lane*, and the same amount of 293 cell extract protein from cells transfected with vector alone was used in the *last lane* (293). The remaining lanes contain varying amounts of purified, recombinant TTP (102–174) peptide, as indicated at the top of the figure. The position of the free RNA probe is indicated. The lane labeled *P* contained the RNA probe without either cytosolic extracts or added recombinant peptide.

To determine binding affinity of TTP73 more quantitatively, we then performed fluorescence anisotropy assays at equilibrium using the same peptide concentrations and the 20-mer oligonucleotide (Fig. 5). In these experiments, solution equilibrium was attained very rapidly ( $< 15$  s). As shown in Fig. 5A, there was no apparent change in fluorescence intensity with different TTP73 concentrations, indicating that the fluorescence quantum yield was not affected by peptide binding. In contrast, anisotropy of the fluorescent 20-mer ARE substrate was dramatically enhanced by the TTP73 peptide (Fig. 5B), and was well described by the Hill model (*solid line*).

The peptide-probe binding occurred with no apparent cooperativity, with a Hill coefficient of  $0.92 \pm 0.05$  (mean  $\pm$  the standard error of regression, defined as one-half of the 95% confidence intervals for each constant). These values are based on data from single experiments containing 40 independent binding reactions; however, duplicate experiments yielded similar results. The Hill coefficient of  $\sim 1$ , coupled with the identification of a single principal protein-RNA complex by the gel shift assay, indicates a binary interaction between a single TTP73 molecule and the 20-mer ARE probe. The association binding constant was  $5.2 \pm 0.3 \times 10^7 \text{ M}^{-1}$ , yielding a  $K_d$  of  $\sim 19$  nM. There was random distribution of residuals (Fig. 5C), indicating no bias for subsets of anisotropy data in the regression solution.

Specificity for the ARE substrate was confirmed by the minimal changes in anisotropy observed for the  $R\beta$  substrate as a function of TTP73 concentration. Slight increases in the anisotropy of the  $R\beta$  substrate for TTP73 concentrations  $> 200$  nM were probably caused by increased sample viscosity at high protein concentrations (24).

**RNA Binding Characteristics of the Biosynthetic, Recombinant TTP (102–174) Peptide**—A peptide of exactly the same sequence as TTP73 was expressed in *Escherichia coli* and purified; this will be referred to as TTP (102–174). Its RNA binding behavior was compared in Fig. 6 with that of the 77-amino acid, epitope-tagged version of the TTP tandem zinc finger domain expressed in 293 cells (11).

A high-speed supernatant fraction of 293 cell cytosol containing this expressed peptide ( $5 \mu\text{g}$  of total cellular protein) shifted the 24-base TNF ARE probe into the same two complexes 1 and 2 noted earlier (Fig. 6, *first and penultimate lanes*, labeled ZF); this is comparable with the shift of a small amount of probe seen with  $5 \mu\text{g}$  of endogenous 293 cell proteins (Fig. 6, *last lane*,

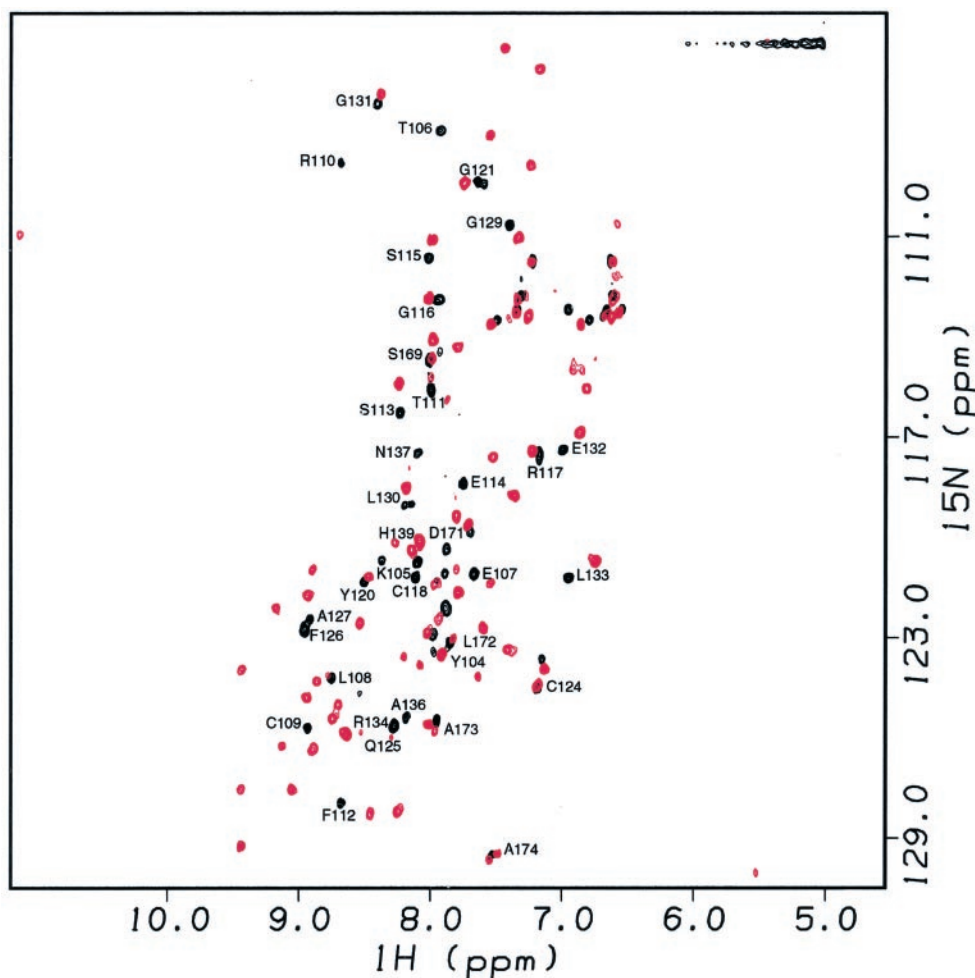


FIG. 7. RNA binding induces the folding of the second zinc finger of TTP.  $^1\text{H}$ - $^{15}\text{N}$  HSQC spectra of free TTP (102–174) (black) and the TTP (102–174)/ARE 17 complex (red) were collected on a Varian Inova 600 MHz NMR spectrometer. Backbone assignments of free TTP (102–174) are labeled. For free TTP (102–174), only 43 of the 69 non-proline residues could be assigned (black); these corresponded to the first zinc finger, a portion of the connecting sequence, and the carboxyl-terminal tail. The numbering system was that used in the GenBank RefSeq NP\_003398. In the presence of a 17-mer ARE RNA oligonucleotide (UUAUUUAUUUAUUUU), resonances of TTP (102–174) were severely perturbed (red); in addition, residues from both zinc fingers of TTP could be accounted for, suggesting that RNA binding induced the folding of the second zinc finger of TTP.

labeled 293). No probe was shifted in the assay buffer alone (Fig. 6, second lane, labeled *P*). The remainder of Fig. 6 shows the effect of the purified recombinant TTP (102–174) peptide on the gel shift assay. At the highest peptide concentrations used, all of the probe was shifted into the gel and formed complex 2 only (40 and 20  $\mu\text{M}$ , Fig. 6). At progressively lower peptide concentrations, there was a gradual decrease in the intensity of complex 2 and an increase in the intensity of complex 1. At the lowest peptide concentration used, 0.04  $\mu\text{M}$ , complex 2 was essentially undetectable, whereas complex 1 was decreased in amount but readily detectable.

These data confirmed that the complex 1 is likely to be formed by occupancy of 1 mol of peptide/mol of probe, and complex 2 results from 2 mol of peptide/mol of probe. As shown above with the synthetic peptide, the apparent affinity of the peptide for the second binding site on the RNA was somewhat lower when the first site was occupied. It is not clear whether this represents an inhibitory effect of the first binding event on the second or one of the two binding sites (*e.g.* 5' versus 3') is superior to the other.

**HSQC Analysis**—HSQC analyses of the  $^{15}\text{N}$ -labeled recombinant peptide showed that essentially all of the amino-terminal amino acids could be accounted for (Fig. 7, resonances colored in black and numbered according to NP\_003398). How-

ever, the residues within the interfinger linker and those of the carboxyl-terminal zinc finger could not be assigned; additional weak resonances could be observed in the  $^1\text{H}$ - $^{15}\text{N}$  HSQC spectra when plotted at the noise level (data not shown).

When the recombinant peptide was titrated with a 17-mer comprising the core ARE sequence, UUAUUUAUUUAUUUAUUU, the HSQC analysis revealed a striking change in the two-dimensional NMR spectrum. There was a dramatic change in the structure of the previously identified amino-terminal residues (Fig. 7, resonances colored in red). In addition, it was now possible to visualize and identify the residues of the carboxyl-terminal half of the peptide, so that residues in both zinc fingers could be accounted for (Fig. 7).

To determine the minimal size of the RNA oligonucleotide that was required to cause this dramatic structural change, we performed similar RNA titrations with two smaller oligonucleotides, basing their sizes on the smallest binding footprint of about 10 bases identified by the gel shift analysis with TTP73. Titration of the  $^{15}\text{N}$ -labeled peptide with the 13-mer RNA oligonucleotide UUAUUUAUUUAUU resulted in the same marked changes in HSQC spectrum as seen with the 17-mer (Fig. 8). Somewhat surprisingly, even the core binding sequence of the 9-mer UUAUUUAUU formed a complex resulting in the same conformation of the peptide (Fig. 8).

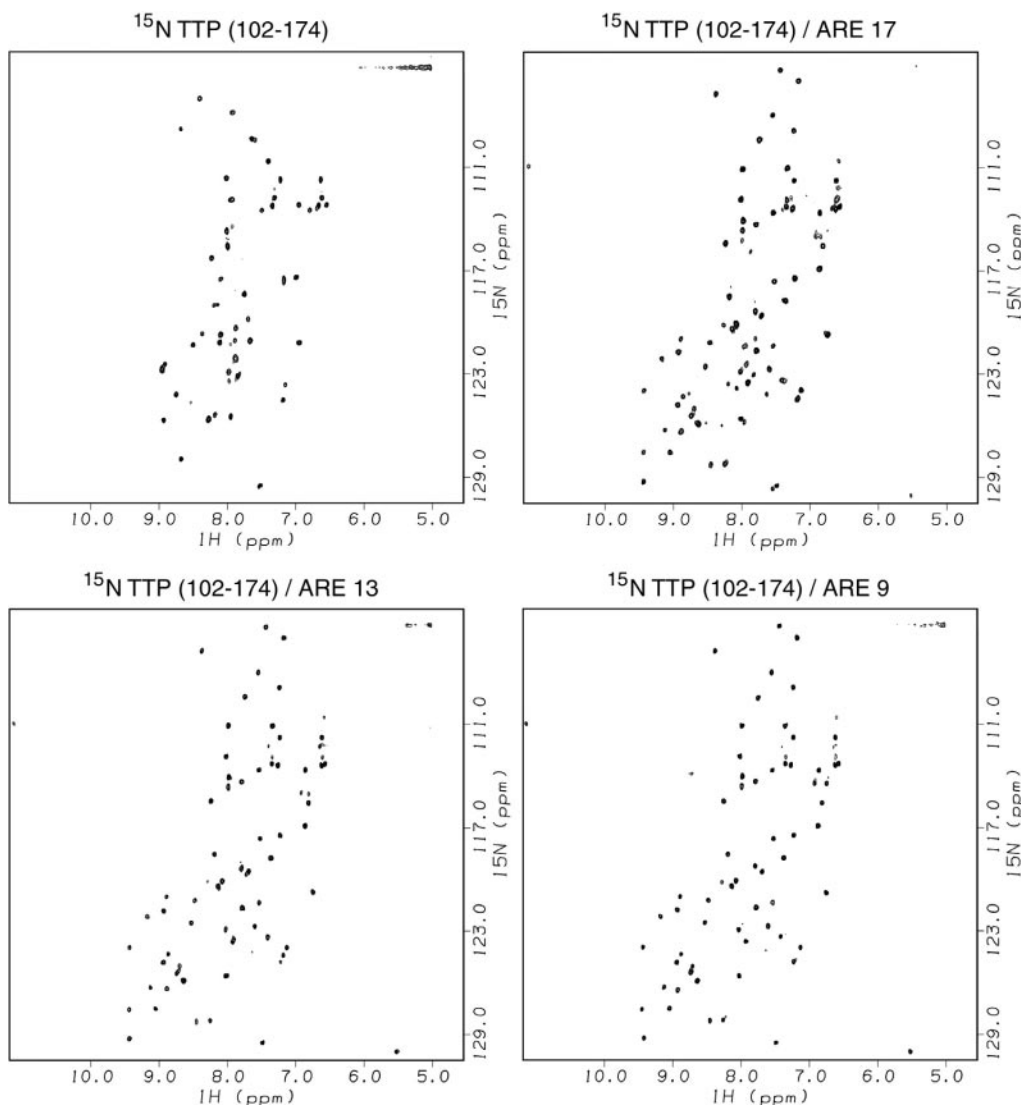


FIG. 8. **ARE 9 contains the core sequence for TTP interaction.** *Top left*, HSQC spectrum of the recombinant  $^{15}\text{N}$ -TTP (102–174) peptide in the absence of added oligonucleotide, as described in Fig. 7. *Top right*, effect of TTP (102–174) in complex with the 17-mer oligonucleotide as described in Fig. 7. *Bottom left*, the effect of titrating in a 13-mer oligonucleotide (UUAUUUAUUUAUU). *Bottom right*, spectrum obtained after titrating in a 9-mer oligonucleotide representing the core ARE (UUAUUUAUU). Note the almost identical spectra obtained in the presence of all three oligonucleotides, all of which are different from the spectrum obtained with the TTP (102–174) peptide alone.

#### DISCUSSION

TTP and its known mammalian relatives, ZFP36L1 and ZFP36L2, have recently been characterized as ARE-binding proteins that lead to the destabilization of the ARE-containing, polyadenylated mRNAs to which they bind. However, the molecular details of the protein-RNA interaction have remained obscure, in part because of difficulties in the bacterial expression of soluble proteins and their RNA binding domains. In an attempt to circumvent some of these expression problems, we designed and chemically synthesized a 73-amino acid peptide composed of the RYKTEL lead-in sequence of the first zinc finger in human TTP, the complete sequences of the two zinc fingers and their 18-amino acid intervening sequence, followed by eight additional carboxyl-terminal residues added in an attempt to promote solubility. This synthetic peptide, TTP73, was readily soluble in aqueous buffers containing low concentrations of zinc and reducing agents at concentrations up to 10 mg/ml. Its ability to bind RNA oligonucleotides representing the core TNF ARE indicated that both zinc fingers were intact, because disruption of only one of several key residues in either zinc finger completely abrogates RNA binding. This peptide

thus seems to be suitable for several types of biochemical study of the protein-RNA interaction, including studies of binding affinity and the effects of other molecules on binding, use in screens for potential drugs that either inhibit or potentiate binding, and ultimately, structural studies of the protein-RNA complex.

During the course of these studies it became apparent that the TTP73 peptide could form more than one complex with ARE probes, as assayed by gel-shift analysis. The number of complexes formed was directly related to the length of the ARE probe used, as well as to the concentration of the peptide. We had previously established that mutating the A residues within the TNF ARE to either G or C residues completely prevented binding of intact TTP, and also interfered with the ability of TTP to promote destabilization of the TNF mRNA in intact cell studies, and the deadenylation of an ARE-containing polyadenylated probe in cell-free studies (11, 14).<sup>2</sup> We therefore used a similar A to C mutation strategy to investigate the formation of multiple complexes between the TTP73 peptide and the wild-type TNF ARE probe.

These studies led to several findings. First, the two com-

plexes formed between the TTP73 peptide and the 24-base ARE probe almost certainly result from tandem occupancy of the probe by two peptide molecules. This portion of the TNF ARE consists of two UUAUUUAUUUA or AUUUUUUUUU 11-mers that are separated by two U residues (underlined) UUAUUUAUUUAUUUAUUUUUUUUUU. It seems likely that the tandem 11-mers are the preferred binding sequence, with the middle UU dimer being less desirable. Still longer oligonucleotides containing an additional binding site could form three complexes, and it seems likely that this in turn was caused by further occupancy of binding sites by additional tandem TTP73 molecules.

The second remarkable finding concerned the size of the TTP73 binding footprint on the ARE probe, as assessed by the A-to-C mutation analysis. Mutations resulting in two, three, or four consecutive A residues (Fig. 3, probes 2, 3, and 5) resulted in the formation of a single peptide-RNA complex, compared with two complexes with the intact probe 1. Mutations resulting in fewer than two consecutive A residues (e.g. Fig. 3, probe 6) exhibited no peptide binding. Remarkably, however, a mutation in which the middle two As were mutated to Cs, leaving two pairs of flanking As (Fig. 3, probe 4), could form two RNA-peptide complexes. These data suggest that the 10-mer sequences UUAUUUAUUU and UUUUUUUUUU could serve as adequate TTP73 binding sites and that the tandem occupancy of probe 4 shown in Fig. 3 was virtually identical to that seen with the wild-type probe 1. Therefore, the range of minimal footprint sizes for TTP73 binding with this set of probes ranged from UUAUUUAUUU or UUUUUUUUUU, both of which bound peptide, to UUAUUU or UUUUUU, both of which failed to bind peptide.

Although so far the mRNAs encoding TNF and GM-CSF are the only ARE-containing mRNAs whose stability has been shown to be regulated by TTP under physiological conditions (i.e. in the TTP knockout mice and/or cells derived from them), the present data have implications for other ARE-containing transcripts potentially regulated by TTP and its related proteins. For example, in the original ARE data base compiled by Khabar and colleagues (25), their groups I–IV include transcripts whose 3'-untranslated regions have five, four, three, and two consecutive AUUUA pentamers, respectively. The number of transcripts in these groups increased dramatically from group I to group IV, with 18 in group I and 175, plus all the transcripts in groups I–III, in group IV. The key characteristic of group IV transcripts is the presence of the WWAUUUAUUUAUU sequence. It seems likely that TTP could bind to this core sequence, thus resulting in a large number of potential mRNA binding partners for TTP and its related proteins in various cells and tissues. These data, however, are limited to TTP73 binding in this cell free system and do not prove that this limited footprint is sufficient to permit either binding of intact TTP or its subsequent mRNA destabilization in cells.

The TTP peptide exhibited a relatively high affinity for the single ARE binding site. Under our gel shift assay conditions, half-maximal peptide binding to a single site on the RNA probe occurred at about 8 nM. A similar value, 2 nM, was seen with a shorter ARE probe and single site binding under different gel shift assay conditions. More quantitative measurement of binding affinity using a single binding site ARE probe and fluorescence anisotropy revealed no cooperativity and a  $K_d$  of ~19 nM under the experimental conditions used. These observations support the conclusion that this peptide-RNA interaction is relatively high affinity. In addition, fluorescence anisotropy represents a practical assay that could be adapted to high-

throughput methods for identifying modifiers of the TTP-RNA interaction.

One of the primary reasons for directly synthesizing a tandem zinc finger domain peptide that was soluble and capable of RNA binding was to develop a reagent that could be used ultimately for structural studies of this peptide-RNA interaction. Such studies have been difficult in the past because of problems with solubility of the recombinant protein and its constituent peptides. Recent studies using a peptide from the mouse TTP tandem zinc finger domain, in which a tyrosine-to-lysine mutation had been created at position 143 of the mouse protein (GenBank accession number NP\_035886), suggested that whereas a structure could be determined for the first zinc finger by NMR methods, a structure could not be solved for the second zinc finger (26, 27). Similarly, in the present studies, the amino acids composing the first zinc finger of the purified recombinant human TTP (102–174) peptide could be assigned, but those of the second zinc finger could not be identified, perhaps because of similar problems to those observed by Berg *et al.* (27) with the mutant mouse peptide. Titration of the TTP (102–174) peptide with an ARE of 17 bases led to a dramatic change in the apparent conformation of the first zinc finger. More surprisingly, the newly formed complex made possible for the first time the assignment of essentially all of the residues in the interfinger linker and in the second zinc finger. An identical conformational shift was also seen with oligonucleotides corresponding to ARE sequences only 13 and 9 bases in length. These data support the previous gel shift data indicating that the binding footprint on the ARE is only about 9 bases. These reagents also may provide the basis for eventual structural studies of the peptide-RNA complex.

*Acknowledgments*—We are grateful to Lu Jiang of Albachem, Ltd., for preparation of the TTP73 peptide and to Paolo Mascagni for helpful suggestions. We also thank Tom Darden and Bob London for critical review of this manuscript and Jeremy Berg for a preprint of Ref. 27.

*Note Added in Proof*—Worthington *et al.* (Worthington, M. T., Pelo, J. W., Sachedina, M. A., Appelgate, J. L., Arseneau, K. O., and Pizarro, T. T. (2002) *J. Biol. Chem.* **277**, 48558–48564) showed recently that recombinant full-length TTP also preferred the extended binding site UUAUUUAUU.

#### REFERENCES

1. Blackshear, P. J. (2001) *Biochem. Soc. Trans.* **30**, 945–952
2. De, J., Lai, W. S., Thorn, J. M., Goldworthy, S. M., Liu, X., Blackwell, T. K., and Blackshear, P. J. (*Gene (Amst.)* **228**, 133–14, 1999)
3. Stevens, C. J., Schipper, H., Samallo, J., Stroband, H. W., and te Kronnie, T. (1998) *Int. J. Dev. Biol.* **42**, 181–188
4. te Kronnie, G., Stroband, H., Schipper, H., and Samallo, J. (1999) *Dev. Genes Evol.* **209**, 443–446
5. Taylor, G. A., Carballo, E., Lee, D. M., Lai, W. S., Thompson, M. J., Patel, D. D., Schenkman, D. I., Gilkeson, G. S., Broxmeyer, H. E., Haynes, B. F., and Blackshear, P. J. (1996) *Immunity* **4**, 445–454
6. Carballo, E., Gilkeson, G. S., and Blackshear, P. J. (1997) *J. Clin. Invest.* **100**, 986–995
7. Carballo, E., Lai, W. S., and Blackshear, P. J. (1998) *Science* **281**, 1001–1005
8. Carballo, E., Lai, W. S., and Blackshear, P. J. (2000) *Blood* **95**, 1891–1899
9. Carballo, E., and Blackshear, P. J. (2001) *Blood* **98**, 2389–2395
10. Lai, W. S., Carballo, E., Strum, J. R., Kennington, E. A., Phillips, R. S., and Blackshear, P. J. (1999) *Mol. Cell. Biol.* **19**, 4311–4323
11. Lai, W. S., Carballo, E., Thorn, J. M., Kennington, E. A., and Blackshear, P. J. (2000) *J. Biol. Chem.* **275**, 17827–17837
12. Lai, W. S., and Blackshear, P. J. (2001) *J. Biol. Chem.* **276**, 23144–23154
13. Lai, W. S., Carballo, E., Thorn, J. M., Kennington, E. A., and Blackshear, P. J. (2000) *J. Biol. Chem.*, **275**, 17827–19837
14. Lai, W. S., Kennington, E. A., and Blackshear, P. J. (2003) *Mol. Cell. Biol.* **23**, 3798–3812
15. Ramage, R., Green, J., Muir, T. W., Ogunjobi, O. M., Love, S., and Shaw, K. (1994) *Biochem. J.* **299**, 151–158
16. Ramage, R., Green, J., and Ogunjobi, O. M. (1989) *Tetrahedron Lett.* **30**, 2149–2152
17. Wilson, G. M., Sutphen, K., Chuang, K. Y., and Brewer, G. (2001) *J. Biol. Chem.* **276**, 8695–8704
18. Wilson, G. M., Sutphen, K., Bolikal, S., Chuang, K. Y., and Brewer, G. (2001) *J. Biol. Chem.* **276**, 44450–44456
19. Lakowicz, J. R. (1999) *Principles of Fluorescence Spectroscopy*, 2nd ed., pp.



- 291–319, Kluwer Academic/Plenum, New York.
20. Wilson, G. M., Sun, Y., Lu, H., and Brewer, G. (1999) *J. Biol. Chem.* **274**, 33374–33381
21. Bartels, C., Xia, T.-H., Billeter, M., Güntert, P., and Wüthrich, K. (1995) *J. Biomol. NMR*, **5**, 1–10
22. Wittekind, M., and Mueller, L. (1993) *J. Magn. Reson. Ser. B* **101**, 201–205
23. Grzesiek, S., and Bax, A. (1992) *J. Am. Chem. Soc.* **114**, 6291–6293
24. Jameson, D. M., and Sawyer, W. H. (1995) *Methods Enzymol.* **246**, 283–300
25. Bakheet, T., Frevel, M., Williams, B. R., Greer, W., and Khabar, K. S. (2001) *Nucleic Acids Res.* **29**, 246–254
26. Worthington, M. T., Amann, B. T., Nathans, D., and Berg, J. M. (1996) *Proc. Natl. Acad. Sci. U. S. A.* **93**, 13754–13759
27. Amann, B. T., Worthington, M. T., and Berg, J. M. (2003) *Biochemistry* **42**, 217–221